

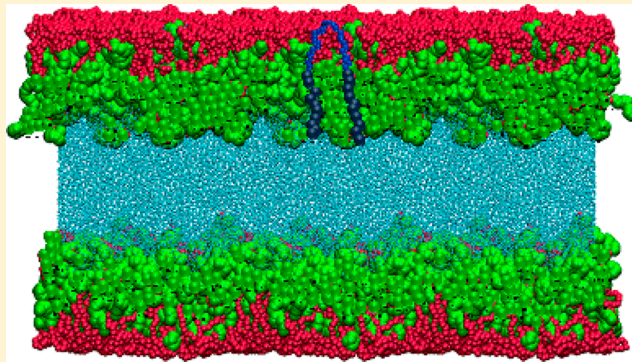
Coarse-Graining Poly(ethylene oxide)–Poly(propylene oxide)–Poly(ethylene oxide) (PEO–PPO–PEO) Block Copolymers Using the MARTINI Force Field

Selina Nawaz* and Paola Carbone*

School of Chemical Engineering and Analytical Science, The University of Manchester, Oxford Road, Manchester, M13 9PL, United Kingdom

Supporting Information

ABSTRACT: The MARTINI coarse-grain (CG) force field is extended for a class of triblock block copolymers known as Pluronics. Existing MARTINI bead types are used to model the non-bonded part of the potential while single chain properties for both homopolymers, poly(ethylene oxide) (PEO) and poly(propylene oxide) (PPO), are used to develop the bonded interactions. The new set of force field parameters reproduces structural and dynamical properties of high molecular weight homo- and copolymers. The CG model is moderately transferable in solvents of different polarity and concentration; however, the PEO homopolymer model presents a reduced thermodynamic transferability especially in water probably due to the lack of hydrogen bonds with the solvent. Our simulations of a monolayer of Pluronic L44 show polymer-brush-like characteristics for the PEO segments which protrude into the aqueous phase. Other membrane properties not easily accessible using experimental techniques such as its membrane thickness are also calculated.



INTRODUCTION

Pluronics is the trademark for a class of amphiphilic linear triblock copolymers consisting of two hydrophilic polyethylene oxide (PEO) blocks connected to a central hydrophobic polypropylene oxide (PPO) block. These copolymers have a wide range of important uses in numerous industrial sectors ranging from cosmetics to more recently medical and pharmaceutical products. They can be used on nanoparticles as a surface coating¹ and even as drug/gene nanocarriers exploiting their ability to self-assemble in polar solvents.² Recently, some Pluronic class copolymers have been shown to enhance gene transcription³ and to have elicit biological responses *in vitro* and *vivo*, showing an increased susceptibility of multi drug resistant cancer cells to chemotherapeutic agents such as doxorubicin.⁴ Experimentally, structural features of Pluronics characterizing their micellar aggregates and mesophases have been studied alongside the effect of temperature on these structural properties.⁵ More recently, due to their potential biological activity, the toxicity of Pluronics of different monomer ratios has also been studied.⁶

Due to the amphiphilic nature of Pluronics, they can self-assemble in polar solvents giving a wide variety of different structures. A typical self-assembling system is a Langmuir monolayer formed by the spread of amphiphiles at the air/water interface. Experimentally, only copolymers with a specific hydrophobic/hydrophilic content can form monolayers at the air/water interface;⁷ therefore, the copolymer rational design is

paramount for their applications.⁸ Experimentally, a range of techniques can be used to study the dynamic and structural properties of Langmuir monolayers over a wide spectrum of dynamical events. For example, it is possible to investigate the monolayer surface activity⁹ and surface pressure using a Langmuir–Blodgett trough.¹⁰ The monolayer thickness and molecular area as a function of surface pressure can also be measured using X-ray and neutron scattering techniques,¹¹ and the study of the molecular conformations of the hydrophobic blocks can be done using infrared and Raman spectroscopy.¹² Despite this wide range of experimental techniques, only molecular based modeling can provide an atomistic resolved picture of the arrangement of the amphiphiles within the self-assembled layer. In this respect, while phospholipid bi- and monolayers have been extensively simulated,¹³ structural and dynamic properties of amphiphilic copolymer monolayers at the air/water interface using molecular simulations have only marginally been studied.¹⁴ This gap in the literature is due to the difficulty in equilibrating and setting up such systems particularly for triblocks such as Pluronics. Computer simulations have helped in clarifying several aspects of the self-assembly properties of amphiphilic block copolymers.¹⁵ Most of these studies employ coarse-grained models^{14,16} or self-

Received: September 15, 2013

Revised: January 15, 2014

Published: January 21, 2014



consistent field techniques,^{14,17} and the use of atomistic resolved models is restricted to the simulations of single chain systems.¹⁸ When the use of atomistic models is prohibitive, the resort of chemical-specific coarse-grained model is the best compromise. Several procedures have been devised in the past decade to develop coarse-grained models that retain specific chemical features of the underlying atomistic structure.¹⁹ Coarse-grained models developed in these ways overcome the time and length scale limitations typical of the atomistic simulations by grouping a cluster of atoms into a single particle or bead. The latter reduces the overall number of particles in the system and also, when employed in molecular dynamics simulations, allowing an increase in the value of the time step. In order to retain the chemical specificities of the system in the model, the procedure to develop the potential interactions acting between the beads may use information coming from both experimental and detailed atomistic simulation data. There are a number of methodologies used for developing CG models for polymers with specific chemical properties. Structure-based CG models²⁰ are quite often used to coarse-grain polymeric systems; however, they have their limitations. For example, Carbone et al. have shown that, while the CG potentials developed targeting structural data (i.e., distance, angle distributions, and radial distribution functions) obtained from detailed atomistic simulations are able to reproduce several system properties, their transferability to thermodynamic states different than those used to perform the atomistic simulations has erratic behavior.²¹

While structural-based models are very popular when isotropic systems are coarse-grained, very few examples of this type of model are present in the literature for the case of amphiphilic molecules which show self-assembly properties. This method has been followed by Bedrov et al. to develop a solvent free coarse-grain model for Pluronics where they utilized a multiscale approach.²² Although the structural-based CG model might be used to coarse-grain polymers in solutions or polymer blends, their use is very limited as ultimately either an additional parametrization of the cross term (solvent–polymer or polymer–polymer) is required or a specific mixing rule has to be sought.^{16d,23} Thermodynamic data properties such as density or surface tension²⁴ can also be used as target properties to develop the force field parameters acting between the coarse-grain beads with limitations to the structural properties. Thermodynamic approaches have been widely used for the modeling of biological environments and amphiphilic molecules and to predict their self-assembly properties.²⁵

The CG force field known as MARTINI is also a thermodynamic based coarse-grain model. It was originally developed specifically for phospholipids forming biological membranes²⁶ but was later extended to model other chemical systems such as proteins,²⁷ carbohydrates,²⁸ and fullerene molecules.²⁹ The parametrization in the MARTINI approach is determined by the reproduction of densities and free energies of partitioning between polar and apolar phases. An advantage of the MARTINI approach is that in multicomponent systems (such as solutions or a protein/lipid bilayer mixture) the parametrization of the cross term (solvent/solute or protein/lipids) non-bonded interactions is a relatively easy task, as the force field consists of simple Lennard-Jones and Coulomb functions. Therefore, the parameters developed for new building blocks can be made compatible with existing MARTINI ones. Recently, Rossi et al.³⁰ and Lee et al.³¹ have

used the MARTINI approach to develop CG models for polymer melts and solution. However, since the structural properties are quite important in modeling polymers, they included in their parametrization procedure some properties targeting mainly the polymer radius of gyration. The percolation of low molecular weight Pluronics through model membranes has recently been seen using the MARTINI force field; however, in this case, the original MARTINI Lennard-Jones parameters have been modified in order to match single chain structural properties compromising the free energy of the system.

In the present work, the development of a MARTINI-compatible CG force field for Pluronics is reported. The force field development uses both thermodynamic and structural data and has been optimized to work with the MARTINI water model.^{26a} The paper is organized as follows: initially, the details of the homopolymer atomistic simulations used to develop the CG force field and the CG molecular dynamics simulations are reported. Then, the CG force field optimization procedure and validation results for the Pluronics are presented followed by structural characterization of a Pluronic Langmuir monolayer at the air/water interface. The conclusions close the paper.

COMPUTATIONAL DETAILS

In order to develop the CG force field, atomistic simulations of a single homopolymer chain of PEO and atactic PPO of various numbers of monomers were performed in SPC type water.³² In addition, simulations of a copolymer test chain composed of 10 monomers of PEO on either side and 10 monomers of PPO in the center ($\text{PEO}_{10}\text{PPO}_{10}\text{PEO}_{10}$) capped with methyl groups were performed in SPC type water.³² Furthermore, atomistic simulations were also performed on some common Pluronic copolymers reported in Table 1. The parametrization of the

Table 1. Characteristics of the Pluronic Copolymers Investigated^a

Pluronic	N_n EO	N_m PO
L31	2	16
L61	3	31
L62	6	31
L64	14	31
L44	10	23
P85	26	40
F38	43	15
F68	75	30

^a N_n represents the number of EO units on each side, and N_m is the number of PO units in the central block of the triblock copolymer.

force field was performed using standard MARTINI water.^{26a} The starting polymer configuration for all the atomistic simulations was obtained by briefly simulating the chain in a vacuum to allow a slight coiling up. The chain was then placed in a box size double the approximated polymer radius of gyration filled with water molecules. The atomistic simulations were performed for 50 ns, and the coarse-grained simulations were run for 1–3 μs depending on the length of the polymer/copolymer chain. Finally, a monolayer of the coarse-grained Pluronic copolymer L44 consisting of 400 copolymer chains arranged 20×20 in the x and y directions with the hydrophilic PEO segments exposed the water region and the hydrophobic PPO toward the vacuum was set up (Figure 1). The monolayer was duplicated and placed across the z -axis. The two

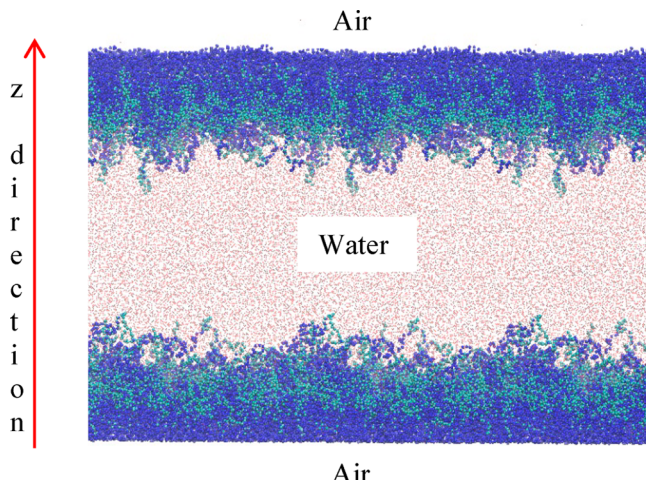


Figure 1. L44 triblock $\text{PEO}_{10}\text{PPO}_{23}\text{PEO}_{10}$ copolymer monolayer. The dark blue beads on the outer edges show the PPO segments of the copolymer, whereas the cyan color beads present the PEO segments. The water is shown as the faded red region in the center.

monolayers facing each other were separated by ~ 20 nm of MARTINI water, and the PPO groups were separated across a periodic boundary of 40 nm of empty space. This duplication of the monolayer is necessary to avoid any water leakage across the box boundary. The monolayer system was simulated for 3 μs . The simulation conditions used to run atomistic and coarse-grain simulations are described in the following sections.

Atomistic Simulations. Molecular dynamics simulations on the all-atom models used parameters from the OPLS-AA force field³³ and were performed using the Gromacs (version 4.5.4) software package.³⁴ A time step of 2 fs was employed, and bonds were constrained using the SHAKE algorithm.³⁵ Long range electrostatics were calculated using the particle mesh Ewald summation (PME)³⁶ with a Fourier spacing of 0.12 nm and a fourth order interpolation. The van der Waals and Coulomb cutoff was set to 1.1 and 0.9 nm, respectively. The neighbor list was updated every 10 steps using a grid with a 0.9 nm cutoff distance. An isothermal-isobaric (*NPT*) ensemble was used to equilibrate all systems maintaining the temperature at 300 K with a Berendsen thermostat and a coupling time of 0.1 ps.³⁷ Isotropic pressure coupling was used for all the systems under investigation using a Berendsen barostat with a reference pressure of 1 bar, coupling time of 1.0 ps, and compressibility of $4.5 \times 10^{-5} \text{ bar}^{-1}$.³⁷

Coarse-Grained Simulations. Coarse-grained simulations were performed using again the Gromacs (version 4.5.4) software package.³⁴ A time step of 20 fs was used, and the neighbor list for the non-bonded interactions was updated every 200 fs. The shift function for dispersion interactions starting from 0.9 nm was used with a cutoff of 1.2 nm. An isothermal-isobaric (*NPT*) ensemble was used to equilibrate all the single chain systems maintaining the temperature at 300 K with a Berendsen thermostat and a coupling time of 0.5 ps.³⁷ Isotropic pressure coupling was used for all the single chain systems under investigation using a Berendsen barostat with a reference pressure of 1.0 bar, coupling time of 4.0 ps, and compressibility of $5.0 \times 10^{-6} \text{ bar}^{-1}$ ³⁷ with the exception to the monolayer system, where surface tension pressure coupling was applied. In this latter case, a reference surface tension value ranging from 0 to 100 dyn/cm was applied in the *xy* plane and

a reference pressure of 1.0 bar was applied along the monolayer normal (*z*-direction).

■ DEVELOPMENT OF THE CG MODEL

The development of the CG force field parameters requires two fundamental choices, the mapping procedure for the coarse-grain particles and the structural or thermodynamic properties targeted in order to validate the model. The mapping procedure involves the selection of the interaction sites that are often chosen arbitrarily. A few attempts have recently been made to automate the mapping procedure.³⁸ For the purpose of this study, each ethylene oxide (EO) and propylene oxide (PO) monomer was mapped as a single coarse-grained particle. The parametrization of the bonded interactions connecting the coarse-grained beads is based on the corresponding pseudointeractions from all-atom simulations performed in this study. The bonded potential includes bond, angle, and dihedral functions, whereas the non-bonded potential is described by Lennard-Jones (LJ) interactions. The energy functions were chosen to be consistent with the MARTINI force field.

Mapping Scheme. The mapping scheme for the Pluronic chain considers the EO and PO monomers as a single particle. MARTINI coarse beads typically consist of four heavy atoms^{26a} with a Lennard-Jones parameter σ of 0.47 nm; more recently, smaller beads have been introduced for cyclic/aromatic structures representing three heavy atoms per bead with σ of 0.43 nm.^{26b} For our Pluronic model, the 3 to 1 mapping scheme is chosen for the mapping procedure. The EO monomer includes three heavy atoms, two methylene groups and an oxygen atom per bead. The PO monomers are formed by four heavy atoms, CH₂, CH, O, and a CH₃ pendant group. Although here there are four heavy atoms in each bead, only three of them are incorporated in the backbone and therefore again a smaller bead type is selected. The chosen mapping scheme is reported in Figure 2.



Figure 2. Superposed description of an atomistic and coarse-grain sample of a Pluronic molecule. The lighter outer and darker central CG beads represent the PEO and PPO segments, respectively.

Parameterization of the Bonded Part of the CG Potential. The parametrization of the bonded interactions for the copolymer chain was performed using distance, angle, and dihedral distributions obtained from the atomistic simulations of the homopolymer chains. The oxygen atom of the EO monomer and the carbon atom of the CH group of the PO were used to calculate the distance, angle, and dihedral distributions (Figure 3). Harmonic functions and a series of cosines were used to fit distance and angle distributions and dihedral distributions, respectively. The force constants were tuned until the atomistic distributions were reproduced by the coarse-grained simulations. (see Figure 3 and Table 2). The dihedral distribution for PEO we obtained from atomistic simulations agrees with the distribution obtained by Lee et al. for the PEO homopolymers.³¹ We then run a simulation of a dummy Pluronic chain consisting of $\text{PEO}_{10}\text{PPO}_{10}\text{PEO}_{10}$ using again both atomistic and coarse models. The bond distance and angle distributions for the interconnecting beads between the PEO and PPO parts of the Pluronics were matched using the same procedure described above (Figure 4).

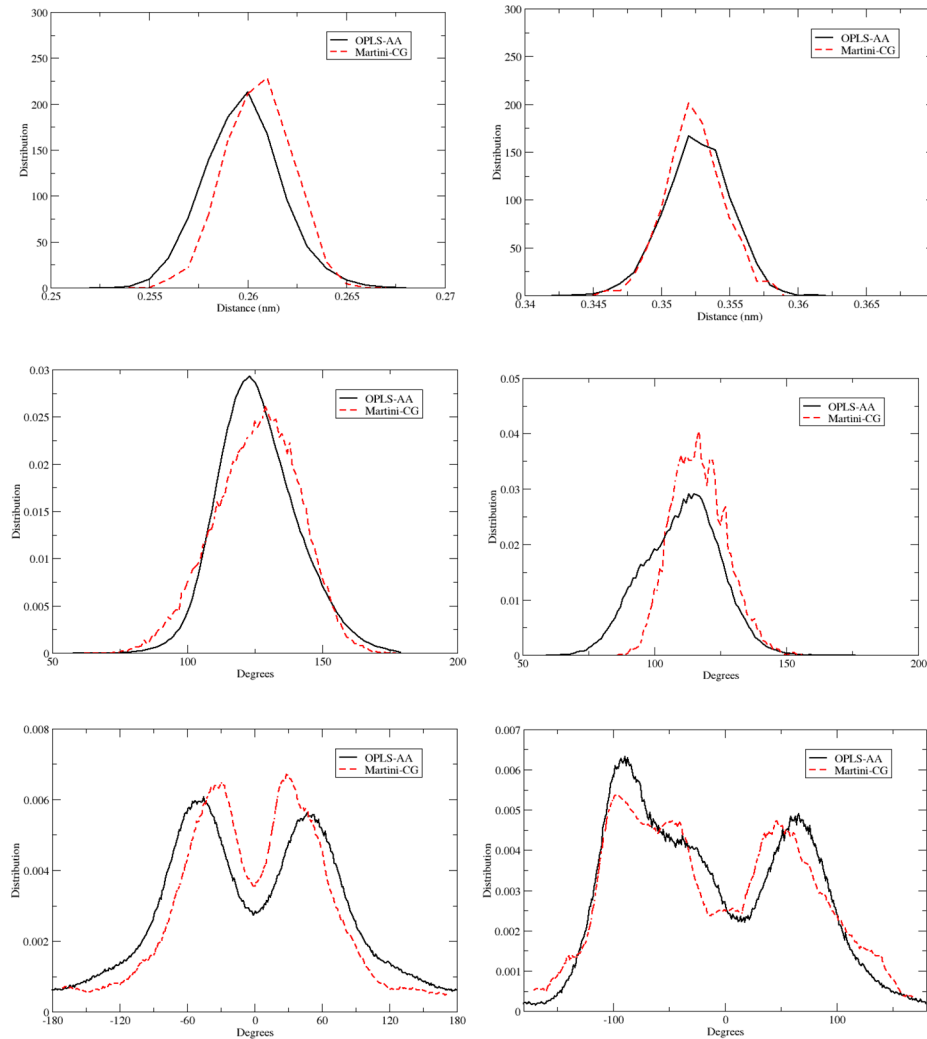


Figure 3. PEO bond distance distribution (top left), PEO angle distribution (middle left), PEO dihedral distribution (bottom left), PPO bond distance distribution (top right), PPO angle distribution (middle right), and PPO dihedral distribution (bottom right).

Table 2. Parameters for the Bonded Interactions for CG Pluronics^a

	bond	K_b (kJ mol ⁻¹ nm ⁻²)	angle	K_θ (kJ mol ⁻¹)	dihedral	K_Φ (kJ mol ⁻¹)	N
	b_0 (Å)		Θ_0 (deg)		Φ_0 (deg)		
EO–EO	0.265	17000	115	50	180	1.96	1
					0	0.18	2
					0	0.33	3
					0	0.12	4
PO–PO	0.355	17000	120	50	180	1.96	1
					0	5.00	2
					0	0.33	3
					0	0.12	4
EO–PO	0.355	17000	120	50			

^aThe functions employed to model the stretching (V_{bond}), bending (V_{angle}), and dihedral (V_{dihedral}) potentials are $V_{\text{bond}}(b) = (1/2)K_b(b - b_0)^2$, $V_{\text{angle}}(\theta) = (1/2)K_\theta(\cos(\theta) - \cos(\theta_0))^2$, and $V_{\text{dihedral}}(\phi) = \sum_{i=1}^m K_\phi(1 + \cos(n_i\phi - \phi_i))$.

Parameterization of the Non-Bonded Part of the CG Potential. The MARTINI procedure develops the non-bonded parameters ϵ and σ using experimental or calculated values of the partition coefficient between octanol and water of small organic molecules resembling the CG beads. This means that in order to not alter the interfacial properties of the CG model those parameters should not be modified during the optimization of the bonded part of the potential. The

experimental partition coefficients, between octanol and water for dimers of PEO (1,2-dimethoxyethane) and PPO (1,2-dimethoxypropane), are 0.21 and 1.78, respectively,^{25b,39} while the values calculated using atomistic molecular simulations are 0.28 and 1.57, respectively.⁴⁰ Among the available MARTINI bead types, for the EO bead, we chose that recently proposed by Rossi et al.,⁴¹ while for the PO bead the existing bead type with the partition coefficient more similar to the PO dimer is

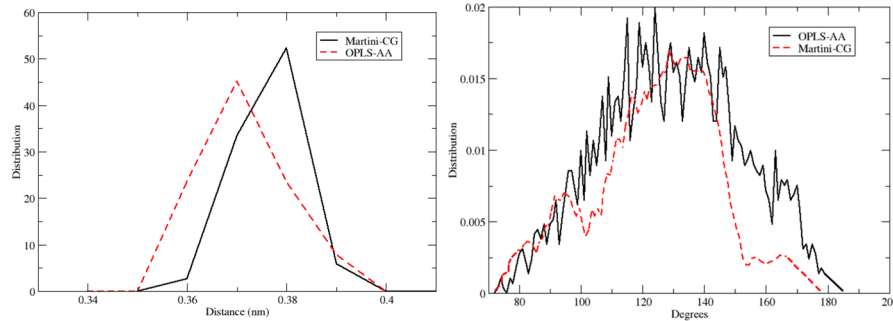


Figure 4. $\text{PEO}_{10}\text{PPO}_{10}\text{PEO}_{10}$ bond distance distribution (left) and $\text{PEO}_{10}\text{PPO}_{10}\text{PEO}_{10}$ angle distribution (right).

that named NO which has a free energy of transfer equal to 5 kJ/mol closely matching the free energy of transfer for the experimentally calculated PPO dimer which is 4.4 kJ/mol.³⁹ The Lennard-Jones parameters for the corresponding beads to PPO and PEO are reported in Table 3.

Table 3. Non-Bonded Interactions for CG Pluronic Beads

	σ (Å)	ϵ (kJ mol ⁻¹)
PEO–PEO	4.3	3.375
PPO–PPO	4.3	2.625
PEO–PPO	4.3	3.750
PEO–W	4.7	3.190
PPO–W	4.7	2.625

RESULTS AND DISCUSSION

Homopolymer Model. Structural Properties. To begin with the validation of the homopolymer PEO and PPO coarse-grained models, various lengths of the homopolymer chains were simulated in water. The corresponding values of the radius of gyration (R_g) were compared favorably with atomistic results obtained for the same polymer lengths (see Table 4).

Table 4. Radius of Gyration Data for PEO and PPO Homopolymers at 300 K

number of PEO/PPO monomers	radius of gyration R_g (nm) OPLS-AA	radius of gyration R_g (nm) MARTINI
30 (PEO)	0.93 ± 0.17	0.83 ± 0.11
60 (PEO)	1.43 ± 0.20	1.34 ± 0.21
90 (PEO)	1.99 ± 0.24	1.71 ± 0.29
30 (PPO)	0.98 ± 0.16	0.92 ± 0.14
60 (PPO)	1.24 ± 0.15	1.40 ± 0.17
90 (PPO)	1.32 ± 0.15	1.56 ± 0.20

Using the CG model, the radii of gyration of several other homopolymers (see Tables 1S and 2S, Supporting Information) were calculated and plotted (Figures 5 and 6) against the polymer molecular weights (specifically the number of monomers). The resulting plot was then fitted by an exponential function:

$$R_g = aM_w^\nu \quad (1)$$

where M_w is the molecular weight in number of monomers and ν is the Flory exponent.

The fitting parameters for our MARTINI PEO model, a and ν , turn out to be $a = 0.088$ and $\nu = 0.65$. These values clearly indicate that the polymer chain is in a good solvent. Previous

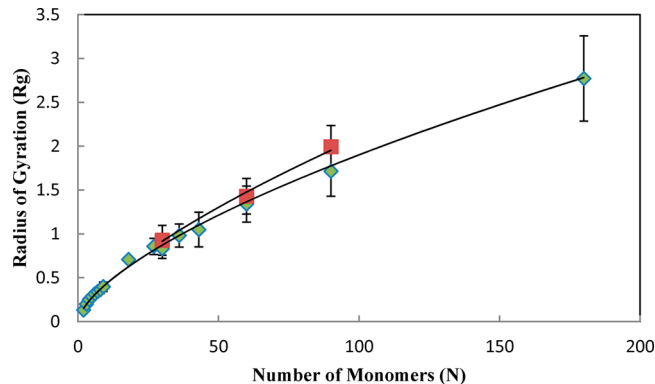


Figure 5. Radius of gyration versus the number of PEO monomers for all-atom simulations (squares) and MARTINI coarse-grain simulations (diamonds). The data are fitted using the exponential function (solid black line) reported in the text.

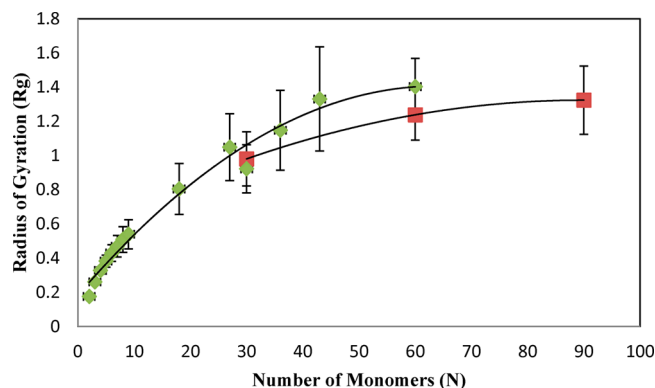


Figure 6. Radius of gyration versus the number of PPO monomers for all-atom simulations (squares) and MARTINI coarse-grain simulations (diamonds). The data are fitted using the exponential function (solid black line) reported in the text.

atomistic simulations of PEO simulations of polymer chains ranging from 18 to 43 monomers^{18a} have predicted a value of $\nu = 0.59$, while experimental light scattering data for larger molecular weights have shown $\nu = 0.6719$, agreeing very well with our coarse-grained results which could reach M_w comparable with the experimental ones.

The fitting parameters for PPO, a and ν , were calculated to be $a = 0.17$ and $\nu = 0.49$. These values indicate that water is a poor solvent for PPO at this temperature and M_w . Atomistic simulations of PPO simulations of polymer chains ranging from 18 to 43 monomers by Hezaveh et al. have resulted in a ν value of 0.5.^{18a} Hezaveh et al. have also observed that the solubility of

the PPO is affected by its chain length in different solvents as a consequence of the change (increase) of its hydrophobicity with the polymer M_w .^{18a} Therefore, our smaller value of v is probably related to the higher M_w we could reach with the CG approach.

The Flory characteristic ratio C_n for a polymer is defined as

$$C_n = \frac{R_{ee}^2}{Nl_b^2} \quad (2)$$

where R_{ee} is the end-to-end distance, N is the number of bonds along the chain, and l_b is the bond length. The Flory characteristic ratio reaches a plateau value known as C_∞ , for large value of N . The value of C_n calculated for the PEO homopolymer is reported in Figure 7.

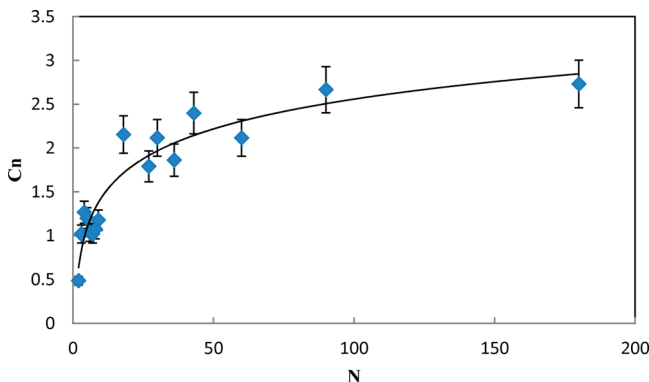


Figure 7. Flory characteristic ratio (C_n) calculated from end-to-end distances versus the number of monomers for the MARTINI force field for PEO monomers.

Using the Flory characteristic ratio C_∞ , the persistence length can be calculated using the following relationship:

$$C_\infty = \frac{2l_p}{l_b} \quad (3)$$

where l_p is the persistence length and l_b is the averaged bond length.

For the PEO MARTINI model using eq 3, a persistence length of 3.7 Å is calculated from a C_∞ value of 2.7 and l_b value of 2.7 Å. This persistence length value correlates well with the experimental value of 3.7 Å for PEO by Mark and Flory.⁴² The persistence length for PPO homopolymers calculated from the characteristic ratio (Figure 8) is 4.0 Å which can be well compared with the value obtained by the atomistic model of Hezaveh et al.^{18a} which predicts a value of 3.75 Å.

Temperature Transferability of the MARTINI Model. There is no guarantee that any chemical specific CG force field is transferable over chemical and thermodynamic states different than that used to develop it, and this transferability needs to be verified case by case.²¹ For the present model, the force field parametrization process was carried out at 300 K; thus, to test whether the force field parameters are transferable, the structural properties of the homopolymer, i.e., the R_g , were calculated at different temperatures. Experimentally, there are indications that both PEO and PPO are hydrophilic at low temperatures. For example, Mortensen has shown that at 278 K both PEO and PPO exist as single polymer chains known as unimers; however, at higher temperatures, PPO becomes more hydrophobic.^{5a} Thus, the first test we did was to check whether

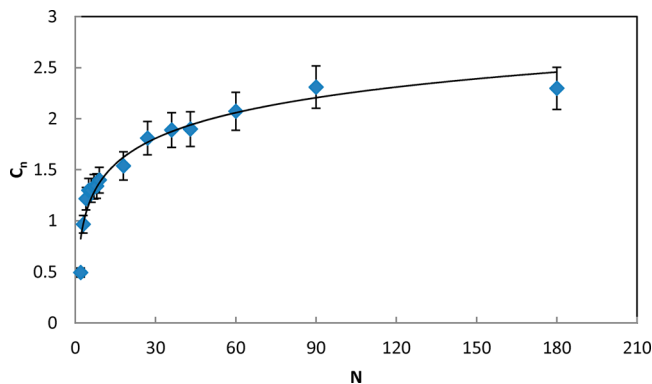


Figure 8. Flory characteristic ratio (C_n) calculated from end-to-end distances versus the number of monomers of PPO using the MARTINI force field.

the temperature has any effects on our atomistic model and then compared the results with the CG ones assuming that the change in hydrophobic character of the homopolymers can be detected by a change in R_g value.

Table 5 compares the R_g values obtained from the atomistic and CG simulations over a wide temperature range (10–60

Table 5. The Radius of Gyration (R_g) of PEO30 in All-Atom Simulations and MARTINI Coarse-Grain Simulations over a Range of Temperatures

temperature (°C)	radius of gyration R_g (nm) OPLS-AA	radius of gyration R_g (nm) MARTINI
10	0.86 ± 0.16	0.92 ± 0.17
20	0.86 ± 0.18	0.90 ± 0.15
30	0.87 ± 0.16	0.92 ± 0.15
40	0.94 ± 0.17	0.92 ± 0.15
50	0.94 ± 0.18	0.92 ± 0.16
60	0.93 ± 0.17	0.92 ± 0.15

°C). The values obtained from the atomistic model (first column) show a moderate increase in the mean value of the R_g with increasing temperature at least up to $T = 40$ °C, although the large standard deviation associated with each value makes it difficult to identify a clear trend. The CG model, on the contrary, presents the same mean value for all the temperatures. This lack of transferability of the force field could be due to the fact that the MARTINI water model used here does not allow formation of hydrogen bonds with the PEO chain, while the atomistic model can easily form such non-bonded interactions.

The homopolymer PPO consisting of 30 monomers was also tested over a wide range of temperatures to observe the effect on the polymer chain (Table 6). In this case, the R_g value of the

Table 6. The Radius of Gyration (R_g) of 30-mer PPO in All-Atom Simulations and MARTINI Coarse-Grain Simulations over a Range of Temperatures

temperature (°C)	radius of gyration R_g (nm) OPLS-AA	radius of gyration R_g (nm) MARTINI
10	0.98 ± 0.16	0.97 ± 0.17
20	0.97 ± 0.16	0.98 ± 0.19
30	0.98 ± 0.14	1.01 ± 0.18
40	0.97 ± 0.16	1.03 ± 0.17
50	0.98 ± 0.15	1.00 ± 0.18
60	0.99 ± 0.14	1.02 ± 0.18

atomistic model is almost constant within the whole temperature range studied. The MARTINI model shows a moderate increase in R_g for the two lowest temperatures above which the R_g value reaches a plateau. As in the case of PEO, all the R_g values present a relatively large statistical error; however, in this case, the lack of any trend in the atomistic results might indicate that, for the hydrophobic PPO polymer, the coarse-grained force field might be used at temperatures different than that used to develop it.

Solvents can play a major role in the polymer configuration. Depending on the chemical nature of the solvent, polymer chains can either collapse to a globule state or swell in an extended conformation and the solvent is classified as poor or good, respectively. The use of the MARTINI force field has the advantage that several beads which might be used to represent solvents are already available in the database. Although the parametrization of our polymers is performed in water, we tested the transferability of the PEO and PPO homopolymers in hexane modeled by SC1 bead type from the original MARTINI parametrization.^{26b} The agreement between the MARTINI and all-atom model is very good for the PPO case (see Table 7) and shows that the force field is clearly

Table 7. Radius of Gyration (R_g) Values for Three Different Lengths of PEO and PPO in Hexane for the All-Atom and MARTINI Coarse-Grain Simulations

number of PEO/PPO monomers	radius of gyration (nm) OPLS-AA	radius of gyration (nm) MARTINI
30 (PEO)	0.71 ± 0.08	0.57 ± 0.05
60 (PEO)	1.10 ± 0.23	0.71 ± 0.04
90 (PEO)	1.56 ± 0.14	1.41 ± 0.04
30 (PPO)	0.96 ± 0.16	0.96 ± 0.16
60 (PPO)	1.10 ± 0.04	1.14 ± 0.04
90 (PPO)	1.33 ± 0.05	1.30 ± 0.08

transferable between different solvents. Less good agreement, especially for low M_w , can instead be observed for the PEO homopolymer, for which the MARTINI model predicts a slightly smaller chain size.

The dynamics of the PEO and PPO homopolymers in the two different chemical environments, polar (water) and apolar (hexane), was also determined by calculating the relaxation times associated with the end-to-end vector \mathbf{R}_{ee} . To do this, the autocorrelation functions $C(t)$ of the end-to-end vector \mathbf{R}_{ee} were calculated:

$$C(t) = \frac{\langle \mathbf{R}_{ee}(0) \cdot \mathbf{R}_{ee}(t) \rangle}{\langle \mathbf{R}_{ee}^2 \rangle} \quad (4)$$

In order to obtain the relaxation time τ , $C(t)$ was fitted using the Kohlrausch–William–Watts stretched exponential functional form:

$$C(t) = \exp[-(t/\alpha)^\beta] \quad (5)$$

where α and β are two fitting parameters and t is the time.

The relaxation time was determined from the numerical integral of the stretched exponential. The autocorrelation functions for the PEO and PPO in water (Figures 9–12) show that the PPO homopolymer is characterized by a longer relaxation time in both solvents than the corresponding PEO homopolymer (Table 8 and 9), as also previously seen in atomistic studies.^{18a} The relaxation times for the MARTINI model are compared with that obtained from all atom models

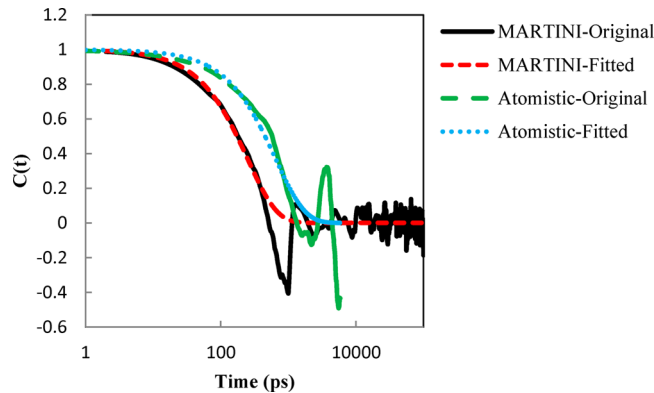


Figure 9. Autocorrelation function ($C(t)$) for PPO30 in water and fitting using eq 7.

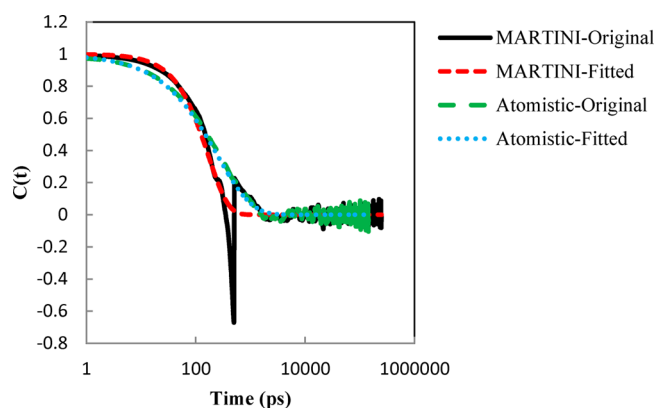


Figure 10. Autocorrelation function for PEO30 in water and fitting using eq 7.

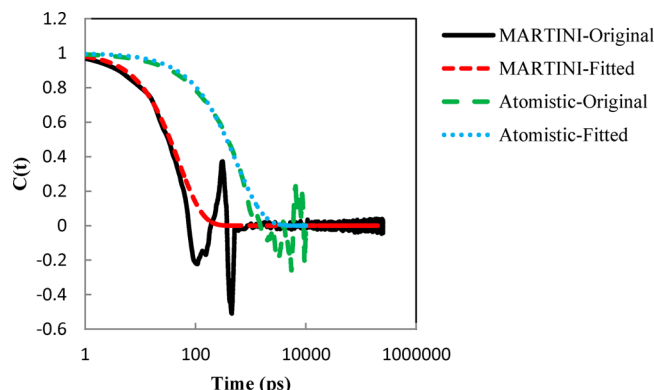


Figure 11. Autocorrelation function for PPO30 in hexane and fitting using eq 7.

for the same homopolymers. From the fitting, it could be clearly seen that both the atomistic and CG models follow the same relaxation mechanism; however, as expected, the polymer relaxes sooner when modeled with the MARTINI force field than with the all-atom one.⁴³ Surprisingly, the best agreement with the atomistic model results is obtained for the simulations performed in water where the difference in relaxation time between the PEO and PPO is correctly reproduced by the MARTINI model. In the case of the simulations performed in hexane instead, the MARTINI model predicts a similar relaxation time for PEO and PPO while the atomistic

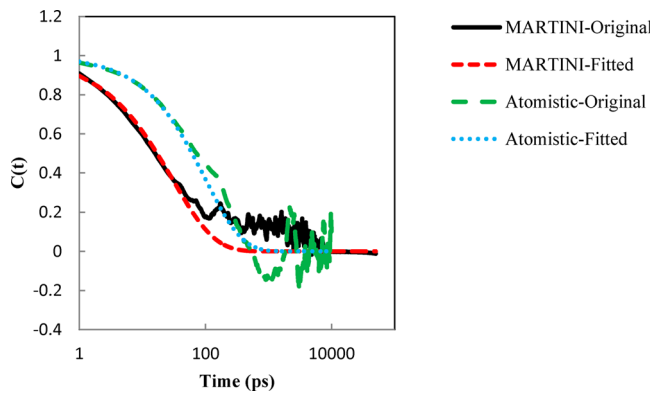


Figure 12. Autocorrelation function for PEO30 in hexane and fitting using eq 7.

Table 8. Relaxation Times for PPO30 and PEO30 in Water

homopolymers in water	relaxation time (ps)
PPO MARTINI	251
PPO atomistic	649
PEO MARTINI	160
PEO atomistic	317

Table 9. Relaxation Times for PPO30 and PEO30 in Hexane

homopolymers in hexane	relaxation time (ps)
PPO MARTINI	49
PPO atomistic	579
PEO MARTINI	41
PEO atomistic	119

simulations show that the PPO should be characterized by a slower relaxation.

Copolymer Model. Structural Properties of the Single Chain. Using the MARTINI bonded parameters developed for the homopolymers, a series of Pluronics molecules (see Table 1) have been built. The model validation in water has been carried out again comparing the single chain size (Table 10).

Table 10. Radius of Gyration Data (in nm) for Pluronics at 300 K (for the Model Labels, See Table 1)

model	OPLS-AA	MARTINI	Gaussian	worm-like
L31	0.79 ± 0.09	0.90 ± 0.25	0.95	0.88
L61	1.16 ± 0.17	1.30 ± 0.25	1.29	1.24
L62	1.27 ± 0.17	1.33 ± 0.26	1.39	1.35
L64	1.37 ± 0.07	1.32 ± 0.20	1.63	1.59
L44	1.34 ± 0.10	1.35 ± 0.18	1.39	1.35
P85		2.11 ± 0.20	2.03	2.01
F38		3.30 ± 0.24	2.13	2.11
F68		4.12 ± 0.29	2.85	2.84

columns 2 and 3). Here it could clearly be seen that the radius of gyration values obtained from the coarse-grained Pluronics models compare very well with the corresponding all-atom ones especially for the high molecular weight copolymers (L62, L64, and L44).

As it has been postulated that Pluronic unimers dissolved in water behave as a Gaussian chain at low temperatures,^{5a} the computational results are compared with the two theoretical models normally used to predict the behavior of polymers in dilute solution: the ideal Gaussian model, which assumes that

the polymer is a freely jointed chain without any local rigidity, and the worm-like model, where a local rigidity is added to the chain through the definition of the chain persistence length.⁴⁴ For a Gaussian and worm-like chain, the radius of gyration can be calculated using eq 6 or 7, respectively

$$R_g = \sqrt{Lb/6} \quad (6)$$

$$R_g = \sqrt{Lb/6 - b^2/4 + (b^3/4L^2)[L - (1 - e^{-2L/b})b/2]} \quad (7)$$

where L is the contour length which is equal to $L = Nl$, where N is the number of monomers in the Pluronics and l is the monomer length; b is the Kuhn length for the Pluronics, which we take as double the mean value from the PEO and PPO persistence length (0.76 nm from our MARTINI models) (see Table 10 and Figure 13).

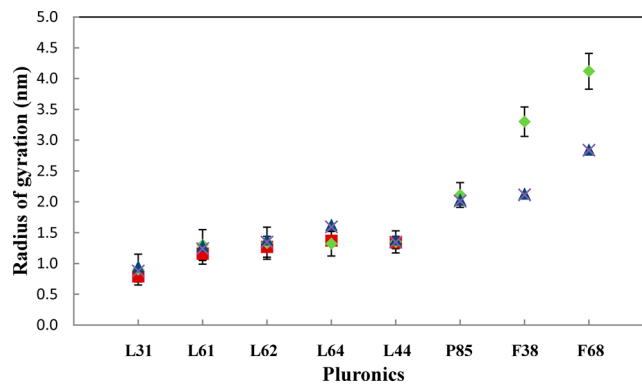


Figure 13. Radius of gyration (R_g) for eight different Pluronics in solution (water) from atomistic simulations (squares), coarse-grain simulations (diamonds), Gaussian chain (triangles), and worm-like chain model predictions (crosses). The data are reported in Table 10.

The two theoretical models predict very similar radii (see Table 10, last two columns). Indeed, the calculated persistence length is relatively small (the monomer length) and the chain results quite flexible. Our calculation confirms^{5a} that the Pluronics behave like a Gaussian chain; however, the ideal model is followed only by low M_w copolymers. The deviation from ideality becomes relevant for copolymers with more than 100 monomers for which the Gaussian model predicts a much lower R_g due to the presence of longer PEO blocks which favorably interact with the water solvent.

Structural Properties of a Preformed Monolayer. Pluronics block copolymers have been recognized as surface active molecules,⁹ and experimentally, a variety of Pluronics have been studied as a Langmuir monolayer. Among the different possible copolymers, L44 ($\text{PEO}_{10}\text{PPO}_{23}\text{PEO}_{10}$) has been extensively studied experimentally in particular as a monolayer at the air/water interface.^{9,45} Its experimental pressure-area ($\pi-A$) isotherm, for example, is well-known and indicates that the monolayer is stable at a surface tension (γ) between 30 and 40 dyn/cm, while for γ above 40 dyn/cm it collapses and forms micellar aggregates.⁹ Although experimentally such systems can be built and studied, the experimental method used to prepare the monolayer can lead to different results^{9,45} and a direct investigation of the structure of the polymer chains within the self-assembled monolayer is not possible and can be achieved only through simulations. Using the MARTINI model developed here, simulations of a preformed monolayer at a

range of different surface tensions have thus been set up and carried out as described in the section “Computational Details” above. As it is known that the use of algorithms which do not explicitly treat the long-range non-bonded Lennard-Jones interactions might result in an underestimation of the experimental surface tension,⁴⁶ the calculation of the entire pressure-area (π - A) isotherm for L44 (Figure 14) was carried

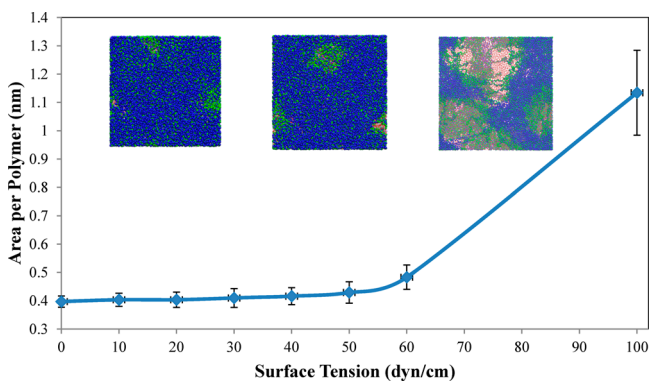


Figure 14. Area per polymer for the L44 block copolymer monolayer at different surface tension values with snapshots of the monolayer taken perpendicular to the membrane normal at the three high surface tension values (50, 60, and 100 dyn/cm) illustrating the membrane rupture and high area per polymer as the surface tension increases.

out. The resulting isotherm helped in identifying the value of the surface tension at which the MARTINI model predicts the monolayer to be stable. In agreement with experiments,⁹ our model predicts an area per polymer almost constant up to $\gamma = 40$ dyn/cm. For values of γ above 40 dyn/cm, the monolayer becomes unstable with formation of pores on the surface and a rapid increase in area per polymer (see snapshots in Figure 14). Therefore, the results presented below, which refer to a stable monolayer, have been obtained from extensive simulations (3 μ s) performed at 37 dyn/cm.

From the simulations, several parameters can be extracted and then compared with the experimental data as, for example, the packing area per polymer which is easily accessible from the experimental π - A isotherm. In simulations, the area per polymer is calculated from the cross-sectional area of the simulation box divided by the total number of polymers per monolayer in the system. Experimentally, Langmuir monolayers of systems that resemble ours have shown an area per polymer value in the range 0.5–1.52 nm². Alexandridis et al.⁹ found that the surface area per copolymer molecule, A , increased as a function of the number of EO segments, N_{EO} , obeying the scaling law $A \approx N_{\text{EO}}^{1/2}$, which is similar to that of lower molecular weight non-ionic surfactants (C_xE_y).⁹ From our simulations at 37 dyn/cm, we observed an area per polymer of 0.405 nm² which compares well with the scaling law predicted by Alexandridis et al. ($A \approx N_{\text{EO}}^{1/2} = 0.447$ nm²). It is also interesting to verify whether the polymer–polymer interactions in monolayer systems lead to a polymer brush behavior similar to that shown by the classic polymer brushes where polymer chains are grafted to a solid surface. In particular, it is known that PEO can form polymer brushes as the grafting density increases.⁴⁷ One important relationship for polymer brushes is that which correlates the brush thickness (h) with the polymer grafting density (σ) via the power scaling law $h \sim \sigma^n$. As the polymer grafting/spacing decreases below the polymer radius of gyration, the exponent n can change from $n = 0$ to $n = 1/3$

(mushroom to brush transition). In the present case, if we consider the polymer height (h) as the thickness of the PEO blocks of our monolayer, which can be calculated from the PEO monomer partial density distribution (see Figure 16), and the grafting density σ as the area per polymer, our monolayer is characterized by a value of $n = 1.4$. This value of n corresponds to a high density brush-like behavior and indicates that the PEO polymer blocks are extended into the water phase. An examination of the dihedral distributions of the PEO segments in the monolayer at the air/water interface further proves this polymer-brush-like behavior. The distribution (Figure 15)

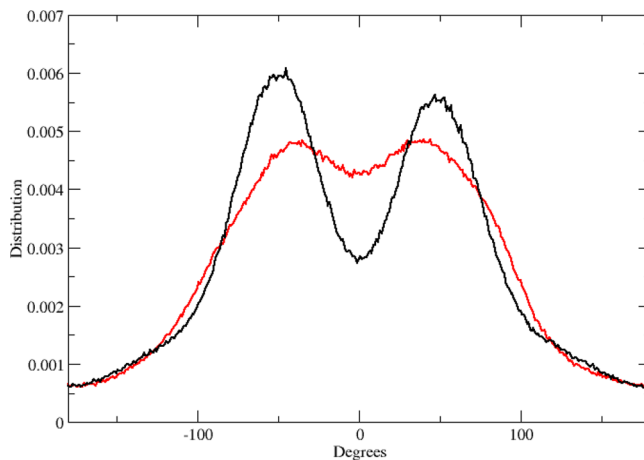


Figure 15. Dihedral distribution for poly(ethylene oxide) (PEO) calculated between the PEO beads. The solid black line represents the dihedral distribution for a single chain of PEO in water. The red line illustrates the dihedral distribution for the PEO segment in the monolayer at a surface tension of 37 dyn/cm.

shows a decrease in the population of the torsional angle at 60° and a corresponding increase in that at 180°, indicating that the PEO chains assume an extended configuration when they are packed in a monolayer structure.

One reason for studying amphiphilic block copolymer membranes using simulations is to enable the identification of properties otherwise not accessible from experiments. The density distribution of particular parts of the system under investigation enables us to determine fundamental properties such as the thickness of a particular layer and penetration of solvent across these layers. For our L44 monolayer, the partial density distribution across the monolayer normal is reported in Figure 16. Closely inspecting this plot, the thickness of the L44 monolayer can be clearly identified to be around 12.3 nm. The difference in the PEO and PPO thickness can also be seen; the PEO segment has a thickness of 9.0 nm, whereas the PPO has a thickness of 10.2 nm. It can clearly be observed that the water fully penetrates into the PEO region whereas the PPO is exposed to the air region, minimizing its contact with the water due to reduced polarity. This observation also demonstrates that the triblock PEO–PPO–PEO Pluronic molecules are adopting a U-shape conformation exposing both PEO blocks to the water and the PPO central block toward the vacuum.

SUMMARY AND CONCLUSION

In this work, we have used the MARTINI force field to parametrize a specific family of triblock copolymers, poly(ethylene oxide) (PEO) and poly(propylene oxide) (PPO) block copolymers (PEO–PPO–PEO), known as Pluronics.

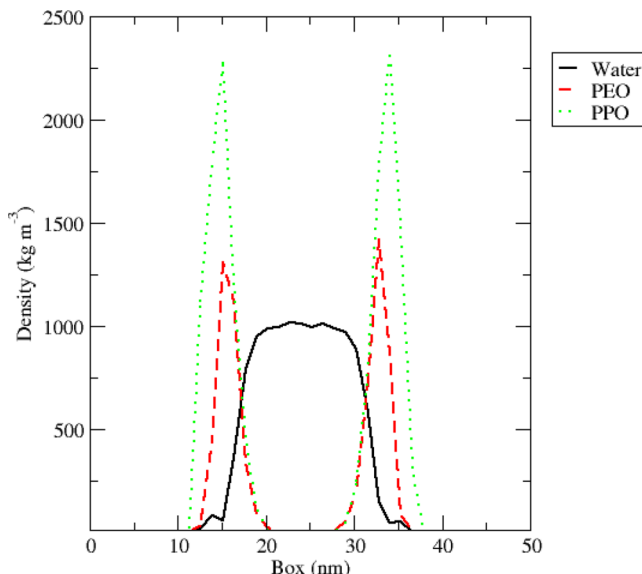


Figure 16. L44 monolayer at the air–water region. The solid black line represents the water in the center of two monolayers. The dashed red line and the dotted green line illustrate the PEO and PPO segments, respectively.

The strategy for the parametrization process has been proven to be a benchmark case for Pluronics of all sizes in different solvents, temperatures, and concentration. We validated the Pluronics model initially separately for the hydrophilic and hydrophobic PEO and PPO components comparing the results with experimental and all-atom simulation data. The PEO blocks have already been validated in a previous study by Rossi et al.;⁴¹ however, further structural parametrization has been performed to validate properties such as radius of gyration, polymer scaling laws, end-to-end distance, persistence length, and relaxation times in solvents of different polarity. The PPO model parametrization involved targeting structural properties after selecting a suitable MARTINI bead type whose free energy of transfer between octanol and water correlates with the experimental value. The parameters developed for the homopolymers have then been used to build the MARTINI model for the copolymers. The missing bonded term for PEO–PPO connection has been targeted to match atomistic bonded parameters. The procedure has been shown to be robust, as structural properties of different Pluronics match well with corresponding all-atom models. A reduced transferability of the force field has been however highlighted especially when the model is tested at temperatures different than that used to parametrize it. In particular, the PEO model does not show any change in its average size when temperature is increased, while in hydrophobic solvent the polymer chain shows a more collapsed configuration than that predicted by the atomistic model. The transferability of the PPO model seems instead more robust. These results indicate that care needs to be taken if phase diagrams of these amphiphilic copolymers are sought or if the thermodynamics of the self-assembly process is investigated in a range of temperatures.

The single chain structural properties have also been compared with theoretical scaling laws. The results show that these models predict correct results only for a subset of Pluronics investigated here, while, for the two polymers with the highest M_w , they greatly underestimate the chain size.

As a test case, a popular Pluronic, L44, monolayer was also simulated using the CG parameters. In order to identify the correct surface tension at which the model predicts the formation of a stable monolayer, a series of simulations at different surface tensions were performed. The entire pressure–area isotherm was built and the correct surface pressure range, which was in agreement with experimental data, identified. Our simulation results indicate that the monolayer shows a brush-like behavior presenting the hydrophilic PEO blocks extended in the water phase and that the proposed scaling law which relates the number of EO units with the area per polymer is followed. Properties not accessible by experimental techniques such as the membrane thickness and conformation of the single polymer chain within the monolayer have also been obtained.

The coarse-grained model developed here reproduces the structural data preserving the original non-bonded interaction parameters of the MARTINI beads, ensuring in this way a reliable prediction of interfacial properties such as copolymer partition coefficients or surface tension. This important model feature should therefore enable the investigation of the copolymer thermodynamic stability at the interface of liquids of different polarity which is a very important factor to be considered when copolymers are used for biological applications or in extraction processes.

ASSOCIATED CONTENT

Supporting Information

The radius of gyration values of 2–180 monomers for PEO using the MARTINI force field are available in Table 1S. The radius of gyration values of 2–43 monomers for PPO using the MARTINI force field are available in Table 2S. This material is available free of charge via the Internet at <http://pubs.acs.org>.

AUTHOR INFORMATION

Corresponding Authors

*E-mail: selina.nawaz@manchester.ac.uk.

*E-mail: paola.carbone@manchester.ac.uk.

Notes

The authors declare no competing financial interest.

ACKNOWLEDGMENTS

The authors would like to show gratitude to Professor Gordon Tiddy for his guidance and support in understanding the experimental data. We also thank Dr. Giulia Rossi and Luca Monticelli for useful discussions on the MARTINI force field. S.N. thanks the EPSRC for financial support through a doctoral prize fellowship.

REFERENCES

- (1) Gaspar, R.; Duncan, R. Polymeric carriers: Preclinical safety and the regulatory implications for design and development of polymer therapeutics. *Adv. Drug Delivery Rev.* 2009, 61 (13), 1220–1231.
- (2) (a) Discher, D. E.; Ahmed, F. Polymersomes. *Annu. Rev. Biomed. Eng.* 2006, 8, 323–41. (b) Adams, M. L.; Lavasanifar, A.; Kwon, G. S. Amphiphilic block copolymers for drug delivery. *J. Pharm. Sci.* 2003, 92 (7), 1343–1355.
- (3) Sriadibhatla, S.; Yang, Z.; Gebhart, C.; Alakhov, V. Y.; Kabanov, A. Transcriptional Activation of Gene Expression by Pluronic Block Copolymers in Stably and Transiently Transfected Cells. *Mol. Ther.* 2006, 13 (4), 804–813.
- (4) Batrakova, E. V.; Li, S.; Brynskikh, A. M.; Sharma, A. K.; Li, Y.; Boska, M.; Gong, N.; Mosley, R. L.; Alakhov, V. Y.; Gendelman, H. E.

- Kabanov, A. V. Effects of pluronic and doxorubicin on drug uptake, cellular metabolism, apoptosis and tumor inhibition in animal models of MDR cancers. *J. Controlled Release* **2010**, *143* (3), 290–301.
- (5) (a) Mortensen, K. Structural studies of aqueous solutions of PEO - PPO - PEO triblock copolymers, their micellar aggregates and mesophases; a small-angle neutron scattering study. *J. Phys.: Condens. Matter* **1996**, *8* (25A), A103. (b) Mortensen, K. Cubic Phase in a Connected Micellar Network of Poly(propylene oxide)-Poly(ethylene oxide)-Poly(propylene oxide) Triblock Copolymers in Water. *Macromolecules* **1997**, *30* (3), 503–507. (c) Mortensen, K.; Batsberg, W.; Hvilsted, S. Effects of PEO-PPO Diblock Impurities on the Cubic Structure of Aqueous PEO-PPO-PEO Pluronics Micelles: fcc and bcc Ordered Structures in F127. *Macromolecules* **2008**, *41* (5), 1720–1727. (d) Mortensen, K.; Talmon, Y. Cryo-TEM and SANS Microstructural Study of Pluronic Polymer Solutions. *Macromolecules* **1995**, *28* (26), 8829–8834. (e) Alexandridis, P.; Nivaggioli, T.; Hatton, T. A. Temperature Effects on Structural Properties of Pluronic P104 and F108 PEO-PPO-PEO Block Copolymer Solutions. *Langmuir* **1995**, *11* (5), 1468–1476. (f) Pedersen, J. S.; Gerstenberg, M. C. The structure of P85 Pluronic block copolymer micelles determined by small-angle neutron scattering. *Colloids Surf., A* **2003**, *213* (2–3), 175–187. (g) Svaneborg, C.; Pedersen, J. S. Form Factors of Block Copolymer Micelles with Excluded-Volume Interactions of the Corona Chains Determined by Monte Carlo Simulations. *Macromolecules* **2001**, *35* (3), 1028–1037.
- (6) Redhead, M.; Mantovani, G.; Nawaz, S.; Carbone, P.; Gorecki, D.; Alexander, C.; Bosquillon, C. Relationship between the Affinity of PEO-PPO-PEO Block Copolymers for Biological Membranes and Their Cellular Effects. *Pharm. Res.* **2012**, *29*, 1908–1918.
- (7) Israelachvili, J. N.; Wennerstroem, H. Entropic forces between amphiphilic surfaces in liquids. *J. Phys. Chem.* **1992**, *96* (2), 520–531.
- (8) (a) Jialanella, G. L.; Firer, E. M.; Piirma, I. Synthesis of polystyrene-block-polyoxyethylene for use as a stabilizer in the emulsion polymerization of styrene. *J. Polym. Sci., Part A: Polym. Chem.* **1992**, *30* (9), 1925–1933. (b) Halperin, A.; Tirrell, M.; Lodge, T. P. Tethered chains in polymer microstructures. *Macromolecules: Synthesis, Order and Advanced Properties*; Springer: Berlin, Heidelberg, 1992; Vol. 100/1, pp 31–71. (c) Alexandridis, P.; Ivanova, R.; Lindman, B. Effect of Glycols on the Self-Assembly of Amphiphilic Block Copolymers in Water. 2. Glycol Location in the Microstructure. *Langmuir* **2000**, *16* (8), 3676–3689. (d) Mouri, E.; Furuya, Y.; Matsumoto, K.; Matsuoka, H. Hydrophilic Chain Length Dependence of the Ionic Amphiphilic Polymer Monolayer Structure at the Air/Water Interface. *Langmuir* **2004**, *20* (19), 8062–8067.
- (9) Yoshioka, S.; Aso, Y.; Kojima, S. Usefulness of the Kohlrausch-Williams-Watts Stretched Exponential Function to Describe Protein Aggregation in Lyophilized Formulations and the Temperature Dependence Near the Glass Transition Temperature. *Pharm. Res.* **2001**, *18* (3), 256–260.
- (10) Mohwald, H. Phospholipid and Phospholipid-Protein Monolayers at the Air/Water Interface. *Annu. Rev. Phys. Chem.* **1990**, *41* (1), 441–476.
- (11) (a) Bayerl, T. M.; Thomas, R. K.; Penfold, J.; Rennie, A.; Sackmann, E. Specular reflection of neutrons at phospholipid monolayers. Changes of monolayer structure and headgroup hydration at the transition from the expanded to the condensed phase state. *Biophys. J.* **1990**, *57* (5), 1095–1098. (b) Brezesinski, G.; Thoma, M.; Struth, B.; Möhwald, H. Structural Changes of Monolayers at the Air/Water Interface Contacted with n-Alkanes. *J. Phys. Chem.* **1996**, *100* (8), 3126–3130.
- (12) Gericke, A.; Moore, D. J.; Erkullu, R. K.; Bittman, R.; Mendelsohn, R. Partially deuterated phospholipids as IR structure probes of conformational order in bulk and monolayer phases. *J. Mol. Struct.* **1996**, *379* (1–3), 227–239.
- (13) (a) Essmann, U.; Perera, L.; Berkowitz, M. L. The Origin of the Hydration Interaction of Lipid Bilayers from MD Simulation of Dipalmitoylphosphatidylcholine Membranes in Gel and Liquid Crystalline Phases. *Langmuir* **1995**, *11* (11), 4519–4531. (b) Chiu, S. W.; Clark, M.; Balaji, V.; Subramaniam, S.; Scott, H. L.; Jakobsson, E. Incorporation of surface tension into molecular dynamics simulation of an interface: a fluid phase lipid bilayer membrane. *Biophys. J.* **1995**, *69* (4), 1230–1245. (c) Egberts, E.; Marrink, S. J.; Berendsen, H. J. C. Molecular-Dynamics Simulation of a Phospholipid Membrane. *Eur. Biophys. J. Biophys. Lett.* **1994**, *22* (6), 423–436. (d) Dominguez, H.; Smolyanov, A. M.; Berkowitz, M. L. Computer Simulations of Phosphatidylcholine Monolayers at Air/Water and CCl₄/Water Interfaces. *J. Phys. Chem. B* **1999**, *103* (44), 9582–9588.
- (14) Daoulas, K.; Müller, M. Comparison of Simulations of Lipid Membranes with Membranes of Block Copolymers. In *Polymer Membranes/Biomembranes*; Meier, W. P., Knoll, W., Eds.; Springer: Berlin, Heidelberg, 2010; Vol. 224, pp 43–85.
- (15) Srinivas, G.; Discher, D. E.; Klein, M. L. *Nat. Mater.* **2004**, *3*, 638.
- (16) (a) Schmid, F. Toy amphiphiles on the computer: What can we learn from generic models? *Macromol. Rapid Commun.* **2009**, *30* (9–10), 741–751. (b) Hatakeyama, M.; Faller, R. Coarse-grained simulations of ABA amphiphilic triblock copolymer solutions in thin films. *Phys. Chem. Chem. Phys.* **2007**, *9* (33), 4662–4672. (c) Sun, Q.; Faller, R. Systematic coarse-graining of atomistic models for simulation of polymeric systems. *Comput. Chem. Eng.* **2005**, *29* (11–12), 2380–2385. (d) Sun, Q.; Pon, F. R.; Faller, R. Multiscale modeling of polystyrene in various environments. *Fluid Phase Equilib.* **2007**, *261* (1–2), 35–40.
- (17) Sevink, G. J. A.; Zvelindovsky, A. V. Self-Assembly of Complex Vesicles. *Macromolecules* **2005**, *38* (17), 7502–7513.
- (18) (a) Hezaveh, S.; Samanta, S.; Milano, G.; Roccatano, D. Molecular dynamics simulation study of solvent effects on conformation and dynamics of polyethylene oxide and polypropylene oxide chains in water and in common organic solvents. *J. Chem. Phys.* **2012**, *136* (12), 124901. (b) Nawaz, S.; Redhead, M.; Mantovani, G.; Alexander, C.; Bosquillon, C.; Carbone, P. Interactions of PEO-PPO-PEO block copolymers with lipid membranes: a computational and experimental study linking membrane lysis with polymer structure. *Soft Matter* **2012**, *8*, 6744–6754.
- (19) Srinivas, G.; Discher, D. E.; Klein, M. L. Self-assembly and properties of diblock copolymers by coarse-grain molecular dynamics. *Nat. Mater.* **2004**, *3* (9), 638–644.
- (20) Karimi-Varzaneh, H. A.; van der Vegt, N. F. A.; Müller-Plathe, F.; Carbone, P. How Good Are Coarse-Grained Polymer Models? A Comparison for Atactic Polystyrene. *ChemPhysChem* **2012**, *13* (15), 3428–3439.
- (21) Carbone, P.; Varzaneh, H. A. K.; Chen, X.; Müller-Plathe, F. Transferability of coarse-grained force fields: The polymer case. *J. Chem. Phys.* **2008**, *128* (6), 064904.
- (22) Bedrov, D.; Ayyagari, C.; Smith, G. D. Multiscale Modeling of Poly(ethylene oxide)-Poly(propylene oxide)-Poly(ethylene oxide) Triblock Copolymer Micelles in Aqueous Solution. *J. Chem. Theory Comput.* **2006**, *2* (3), 598–606.
- (23) (a) Qian, H.-J.; Carbone, P.; Chen, X.; Karimi-Varzaneh, H. A.; Liew, C. C.; Müller-Plathe, F. Temperature-Transferable Coarse-Grained Potentials for Ethylbenzene, Polystyrene, and Their Mixtures. *Macromolecules* **2008**, *41* (24), 9919–9929. (b) Reith, D.; Müller, B.; Müller-Plathe, F.; Wiegand, S. How does the chain extension of poly(acrylic acid) scale in aqueous solution? A combined study with light scattering and computer simulation. *J. Chem. Phys.* **2002**, *116* (20), 9100–9106.
- (24) Nielsen, S. O.; Lopez, C. F.; Srinivas, G.; Klein, M. L. A coarse grain model for n-alkanes parameterized from surface tension data. *J. Chem. Phys.* **2003**, *119* (14), 7043–7049.
- (25) (a) Shelley, J. C.; Shelley, M. Y.; Reeder, R. C.; Bandyopadhyay, S.; Klein, M. L. A Coarse Grain Model for Phospholipid Simulations. *J. Phys. Chem. B* **2001**, *105* (19), 4464–4470. (b) Funasaki, N.; Hada, S.; Neya, S.; Machida, K. Intramolecular hydrophobic association of two alkyl chains of oligoethylene glycol diethers and diesters in water. *J. Phys. Chem.* **1984**, *88* (24), 5786–5790.
- (26) (a) Marrink, S. J.; de Vries, A. H.; Mark, A. E. Coarse Grained Model for Semiquantitative Lipid Simulations. *J. Phys. Chem. B* **2004**, *108* (2), 750–760. (b) Marrink, S. J.; Risselada, H. J.; Yefimov, S.;

- Tieleman, D. P.; de Vries, A. H. The MARTINI Force Field: Coarse Grained Model for Biomolecular Simulations. *J. Phys. Chem. B* **2007**, *111* (27), 7812–7824.
- (27) Monticelli, L.; Kandasamy, S. K.; Periole, X.; Larson, R. G.; Tieleman, D. P.; Marrink, S.-J. The MARTINI Coarse-Grained Force Field: Extension to Proteins. *J. Chem. Theory Comput.* **2008**, *4* (5), 819–834.
- (28) López, C. A.; Rzepiela, A. J.; de Vries, A. H.; Dijkhuizen, L.; Hünenberger, P. H.; Marrink, S. J. Martini Coarse-Grained Force Field: Extension to Carbohydrates. *J. Chem. Theory Comput.* **2009**, *5* (12), 3195–3210.
- (29) Wong-Ekkabut, J.; Baoukina, S.; Triampo, W.; Tang, I. M.; Tieleman, D. P.; Monticelli, L. Computer simulation study of fullerene translocation through lipid membranes. *Nat. Nanotechnol.* **2008**, *3* (6), 363–368.
- (30) Rossi, G.; Monticelli, L.; Puisto, S. R.; Vattulainen, I.; Ala-Nissila, T. Coarse-graining polymers with the MARTINI force-field: polystyrene as a benchmark case. *Soft Matter* **2011**, *7* (2), 698–708.
- (31) Lee, H.; de Vries, A. H.; Marrink, S.-J.; Pastor, R. W. A Coarse-Grained Model for Polyethylene Oxide and Polyethylene Glycol: Conformation and Hydrodynamics. *J. Phys. Chem. B* **2009**, *113* (40), 13186–13194.
- (32) Glattli, A.; Daura, X.; Gunsteren, W. F. v. Derivation of an improved simple point charge model for liquid water: SPC/A and SPC/L. *J. Chem. Phys.* **2002**, *116* (22), 9811–9828.
- (33) Jorgensen, W. L.; Severance, D. L. Aromatic-aromatic interactions: free energy profiles for the benzene dimer in water, chloroform, and liquid benzene. *J. Am. Chem. Soc.* **1990**, *112* (12), 4768–4774.
- (34) Hess, B.; van der Spoel, D.; Lindahl, E.; Apol, E.; Apostolov, R.; Berendsen, H. J. C.; van Buuren, A.; Bjelkmar, P.; van Drunen, R.; Feenstra, A.; Groenhof, G.; Kasson, P.; Larsson, P.; Meulenhoff, P.; Murtola, T.; Páll, S.; Pronk, S.; Schulz, R.; Shirts, M.; Sijbers, A.; Tieleman, P. *Gromacs User Manual*, version 4.5.4; 2010; www.gromacs.org.
- (35) Ryckaert, J.-P.; Ciccotti, G.; Berendsen, H. J. C. Numerical integration of the cartesian equations of motion of a system with constraints: molecular dynamics of n-alkanes. *J. Comput. Phys.* **1977**, *23* (3), 327–341.
- (36) (a) Darden, T.; York, D.; Pedersen, L. Particle mesh Ewald: An N [center-dot] log(N) method for Ewald sums in large systems. *J. Chem. Phys.* **1993**, *98* (12), 10089–10092. (b) Essmann, U.; Perera, L.; Berkowitz, M. L.; Darden, T.; Lee, H.; Pedersen, L. G. A smooth particle mesh Ewald method. *J. Chem. Phys.* **1995**, *103* (19), 8577–8593.
- (37) Berendsen, H. J. C.; Postma, J. P. M.; Gunsteren, W. F. v.; DiNola, A.; Haak, J. R. Molecular dynamics with coupling to an external bath. *J. Chem. Phys.* **1984**, *81* (8), 3684–3690.
- (38) (a) Murtola, T.; Kupiainen, M.; Falck, E.; Vattulainen, I. Conformational analysis of lipid molecules by self-organizing maps. *J. Chem. Phys.* **2007**, *126* (5), 054707. (b) Zhang, Z.; Lu, L.; Noid, W. G.; Krishna, V.; Pfaendtner, J.; Voth, G. A. A Systematic Methodology for Defining Coarse-Grained Sites in Large Biomolecules. *Biophys. J.* **2008**, *95* (11), 5073–5083. (c) Zhang, Z.; Pfaendtner, J.; Grafmüller, A.; Voth, G. A. Defining Coarse-Grained Representations of Large Biomolecules and Biomolecular Complexes from Elastic Network Models. *Biophys. J.* **2009**, *97* (8), 2327–2337. (d) Fraccalvieri, D. *Comparison of protein dynamics: a new methodology based on self-organizing maps*. Università degli Studi di Milano-Bicocca, 2011. (e) Fraccalvieri, D.; Pandini, A.; Stella, F.; Bonati, L. Conformational and functional analysis of molecular dynamics trajectories by Self-Organising Maps. *BMC Bioinf.* **2011**, *12* (1), 158.
- (39) (a) Sangster, J. *Octanol-Water Partition Coefficients: Fundamentals and Physical Chemistry*; Wiley: Chichester, U.K., New York, 1997. (b) Chemicalland21; www.chemicalland21.com.
- (40) Moh, L. C. H.; Losego, M. D.; Braun, P. V. Solvent Quality Effects on Scaling Behavior of Poly(methyl methacrylate) Brushes in the Moderate- and High-Density Regimes. *Langmuir* **2011**, *27* (7), 3698–3702.
- (41) Rossi, G.; Fuchs, P. F. J.; Barnoud, J.; Monticelli, L. A Coarse-Grained Martini Model of Polyethylene Glycol and of Polyoxyethylene Alkyl Ether Surfactants. *J. Phys. Chem. B* **2012**, *116* (49), 14353–14362.
- (42) Mark, J. E.; Flory, P. J. The Configuration of the Polyoxyethylene Chain. *J. Am. Chem. Soc.* **1965**, *87* (7), 1415–1423.
- (43) Hezaveh, S.; Samanta, S.; De Nicola, A.; Milano, G.; Roccatano, D. Understanding the Interaction of Block Copolymers with DMPC Lipid Bilayer Using Coarse-Grained Molecular Dynamics Simulations. *J. Phys. Chem. B* **2012**, *116* (49), 14333–14345.
- (44) Kratky, O.; Porod, G. *Recl. Trav. Chim. Pays-Bas* **1949**, *68*, 1106.
- (45) Naskar, B.; Ghosh, S.; Moulik, S. P. Solution Behavior of Normal and Reverse Triblock Copolymers (Pluronic L44 and 10R5) Individually and in Binary Mixture. *Langmuir* **2012**, *28* (18), 7134–7146.
- (46) Klauda, J. B.; Wu, X.; Pastor, R. W.; Brooks, B. R. Long-Range Lennard-Jones and Electrostatic Interactions in Interfaces: Application of the Isotropic Periodic Sum Method. *J. Phys. Chem. B* **2007**, *111* (17), 4393–4400.
- (47) Bedrov, D.; Smith, G. D. Molecular Dynamics Simulation Study of the Structure of Poly(ethylene oxide) Brushes on Nonpolar Surfaces in Aqueous Solution. *Langmuir* **2006**, *22* (14), 6189–6194.